

# Dissecting Anion Effects in Gold(I)-Catalyzed Intermolecular Cycloadditions

Anna Homs,<sup>+a</sup> Carla Obradors,<sup>+a</sup> David Leboeuf,<sup>a</sup> and Antonio M. Echavarren<sup>a,b,\*</sup>

<sup>a</sup> Institute of Chemical Research of Catalonia (ICIQ), Av. Països Catalans 16, 43007 Tarragona, Spain  
Fax: (+34)-97-792-0225; e-mail: aechavarren@icq.es

<sup>b</sup> Departament de Química Analítica i Química Orgànica, Universitat Rovira i Virgili, C/Marcel·li Domingo s/n, 43007 Tarragona, Spain

<sup>+</sup> These two authors contributed equally to this work.

Received: August 4, 2013; Revised: October 10, 2013; Published online: January 13, 2014

Supporting information for this article is available on the WWW under <http://dx.doi.org/10.1002/adsc.201300704>.

© 2014 The Authors. Published by Wiley-VCH Verlag GmbH & Co. KGaA. This is an open access article under the terms of the Creative Commons Attribution Non-Commercial License, which permits use, distribution and reproduction in any medium, provided the original work is properly cited and is not used for commercial purposes.

**Abstract:** From a series of gold complexes of the type  $[t\text{-BuXPhosAu}(\text{MeCN})]\text{X}$  ( $\text{X} = \text{anion}$ ), the best results in intermolecular gold(I)-catalyzed reactions are obtained with the complex with the bulky and soft anion  $\text{BAR}_4^{\text{F}^-}$  [ $\text{BAR}_4^{\text{F}^-} = 3,5\text{-bis}(\text{trifluoromethyl})\text{phenylborate}$ ] improving the original protocols by 10–30% yield. A kinetic study on the [2+2] cycloaddition reaction of alkynes with alkenes is consistent with an scenario in which the rate-determining step is the ligand exchange to generate the  $(\eta^2\text{-phenylacetylene})\text{gold}(\text{I})$  complex. We have studied in detail the subtle differences that can be attributed to the anion in this formation, which result in a substantial decrease in the formation of unproductive  $\sigma,\pi\text{-(alkyne)digold}(\text{I})$  complexes by destabilizing the conjugated acid formed.

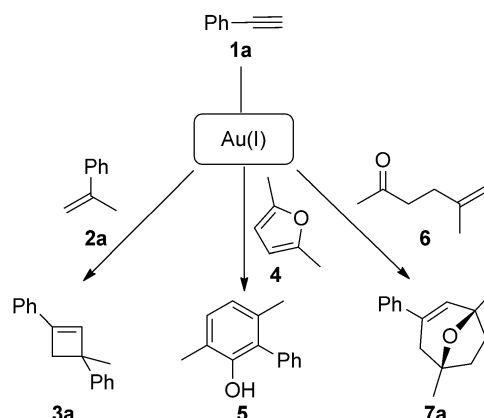
**Keywords:** cycloaddition; cyclobutenes; gold catalysis; mechanistic study

## Introduction

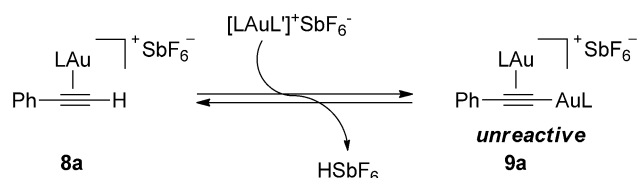
Gold(I)-catalyzed intramolecular cycloisomerization reactions have been widely studied during the last decade.<sup>[1]</sup> Gold(I) complexes have been found to be powerful homogeneous catalysts for carbon-carbon, carbon-oxygen or carbon-nitrogen bond formation proceeding by nucleophilic additions to alkynes,

allenes and alkenes, giving access to new carbo- and heterocyclic compounds. Despite these major advances, the development of intermolecular cycloadditions using alkynes as the substrates has been shown to be challenging.<sup>[2]</sup>

By using cationic gold(I) complexes with bulky ligands, we developed the intermolecular reaction of alkynes with alkenes to form regioselectively cyclobutenes of type **3a** (Scheme 1).<sup>[3,4]</sup> More recently, we have developed a synthesis of phenols **5** by the intermolecular reaction of alkynes with furans such as **4**,<sup>[5,6]</sup> as well as a synthesis of oxabicyclo[3.2.1]oct-3-enes of type **7a** by cycloaddition between oxoalkene **6** and **1a**.<sup>[7]</sup>



**Scheme 1.** Gold(I)-catalyzed intermolecular reactions.



**Scheme 2.** Formation of  $\sigma,\pi$ -digold(I) complexes from ( $\eta^2$ -alkyne)gold(I) complexes ( $L = t\text{-BuXPhos}$ ).

During our studies on the [2+2+2] cycloaddition of alkynes with oxoalkenes,<sup>[7]</sup> we discovered that formation of the active gold species was more complex than expected. Although it was possible to observe the phenylacetylene gold(I) complex (**8a**) at  $-60^\circ\text{C}$ , the resting state under the reaction conditions was the unreactive  $\sigma,\pi$ -(phenylacetylene)digold(I) complex **9a**, which decreases the reaction efficiency (Scheme 2).

Different research groups reported the formation of very similar digold(I) complexes and their influence on the reactivity in catalytic transformations.<sup>[8]</sup> In this context, we have focused on tuning the catalyst structure to minimize the formation of digold(I) complexes. In intermolecular reactions involving alkynes, we reasoned that the use of a more bulky, non-coordinating, and less basic counterion could slow down the deprotonation of terminal alkynes to form the  $\sigma$ -acetylide gold(I) intermediates. Hence, we have prepared the new gold(I) complexes [*t*-BuXPhosAu(MeCN)]BAR<sub>4</sub><sup>F-</sup> **A2** and [IPrAu(PhCN)]BAR<sub>4</sub><sup>F-</sup> **B2** with the BAR<sub>4</sub><sup>F-</sup> anion [BAR<sub>4</sub><sup>F-</sup> = 3,5-bis(trifluoromethyl)phenylborate] (Figure 1).<sup>[9]</sup> These are close relatives

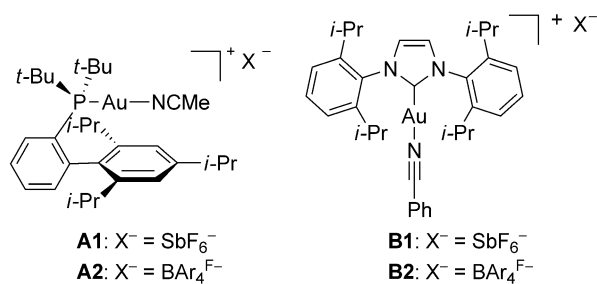


**Figure 1.** Cationic gold(I) complexes with SbF<sub>6</sub><sup>-</sup> and BAR<sub>4</sub><sup>F-</sup> anions (BAR<sub>4</sub><sup>F-</sup> = 3,5-bis(trifluoromethyl)phenylborate).

of the corresponding complexes **A1**<sup>[10]</sup> and **B1**<sup>[11]</sup> with hexafluoroantimonate anion, which have been used as the catalysts of choice in gold(I)-catalyzed intermolecular reactions.<sup>[3,4,5,7]</sup> Since complex **B2** showed slightly better performance than **B1** in the intermolecular synthesis of phenols of type **5**,<sup>[5]</sup> we decided to study in detail the effect of the anion on the corresponding *t*-BuXPhos complexes **A1** and **A2**. Analogous complexes with BF<sub>4</sub><sup>-</sup> and PF<sub>6</sub><sup>-</sup> anions **A3** and **A4** have also been studied. Herein we present a mechanistic

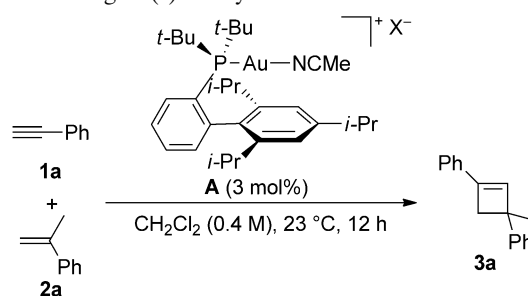
study of the intermolecular [2+2] cycloaddition of alkynes with alkenes in order to understand the influence of the counterion on the reactivity of these processes. This work shows that **A2** is the catalyst of choice for intermolecular reactions of terminal alkynes.

## Results and Discussion

The [2+2] cycloaddition of alkynes with alkenes was developed using complex [*t*-BuXPhosAu(MeCN)]SbF<sub>6</sub> (**A1**) as catalyst, furnishing regioselectively cyclobutenes **3** in moderate to good yields.<sup>[3]</sup> This cycloaddition proceeded under mild conditions in dichloromethane at room temperature. Although, as expected, the ligand had a strong influence on the selectivity, we were surprised by the notable difference observed when changing the counterion (Table 1). Thus, replacing SbF<sub>6</sub><sup>-</sup> in **A1** by BAR<sub>4</sub><sup>F-</sup> (**A2**) leads to an increase in the yield of the cycloaddition of **1a** with **2a** from 80 to 95% (Table 1, entries 1 and 2). The use of BF<sub>4</sub><sup>-</sup>, PF<sub>6</sub><sup>-</sup>, NTf<sub>2</sub><sup>-</sup> or OTf<sup>-</sup> as counterions led to **3a** in lower yields (Table 1, entries 3–6).

The cycloaddition between different terminal alkynes and **2a** using catalysts **A1** and **A2** is shown in Table 2. In most cases, yields using **A2** were 10–30% higher (Table 2), with the exception of MeO-substituted alkynes **1c**, **1g**, and **1i**, which afforded the corresponding cyclobutenes in very similar yields (Table 2,

**Table 1.** Intermolecular gold(I)-catalyzed [2+2] cycloaddition between phenylacetylene (**1a**) and  $\alpha$ -methylstyrene (**2a**) with different gold(I) catalysts **A**.<sup>[a]</sup>



Entry	X <sup>-</sup>	<b>3a</b> (Yield [%]) <sup>[b]</sup>
1	SbF <sub>6</sub> <sup>-</sup>	80
2	BAR <sub>4</sub> <sup>F-</sup>	95
3	BF <sub>4</sub> <sup>-</sup>	62
4	PF <sub>6</sub> <sup>-</sup>	19
5 <sup>[c]</sup>	NTf <sub>2</sub> <sup>-</sup>	26
6 <sup>[c]</sup>	OTf <sup>-</sup>	18

<sup>[a]</sup> **2a/1a** = 2:1.

<sup>[b]</sup> Yield determined by <sup>1</sup>H NMR using 1,4-diacetylbenzene as internal standard.

<sup>[c]</sup> Catalysts generated *in situ* with [LAuCl] and the corresponding silver salts.

**Table 2.** Intermolecular gold(I)-catalyzed [2+2] cycloaddition between alkynes (**1a–n**) and  $\alpha$ -methylstyrene (**2a**).<sup>[a]</sup>

Entry	R	Catalyst	Product (Yield [%]) <sup>[b]</sup>
1	Ph ( <b>1a</b> )	<b>A1</b>	<b>3a</b> (80) <sup>[c]</sup>
2		<b>A2</b>	<b>3a</b> (95)
3	<i>p</i> -Tol ( <b>1b</b> )	<b>A1</b>	<b>3b</b> (74) <sup>[c]</sup>
4		<b>A2</b>	<b>3b</b> (86)
5	<i>p</i> -MeOC <sub>6</sub> H <sub>4</sub> ( <b>1c</b> )	<b>A1</b>	<b>3c</b> (68) <sup>[c]</sup>
6		<b>A2</b>	<b>3c</b> (64)
7	<i>p</i> -FC <sub>6</sub> H <sub>4</sub> ( <b>1d</b> )	<b>A1</b>	<b>3d</b> (75) <sup>[c]</sup>
8		<b>A2</b>	<b>3d</b> (84)
9	<i>p</i> -ClC <sub>6</sub> H <sub>4</sub> ( <b>1e</b> )	<b>A1</b>	<b>3e</b> (61) <sup>[c]</sup>
10		<b>A2</b>	<b>3e</b> (91)
11	<i>p</i> -BrC <sub>6</sub> H <sub>4</sub> ( <b>1f</b> )	<b>A1</b>	<b>3f</b> (74) <sup>[c]</sup>
12		<b>A2</b>	<b>3f</b> (97)
13	<i>m</i> -MeOC <sub>6</sub> H <sub>4</sub> ( <b>1g</b> )	<b>A1</b>	<b>3g</b> (80)
14		<b>A2</b>	<b>3g</b> (78)
15	<i>m</i> -Tol ( <b>1h</b> )	<b>A1</b>	<b>3h</b> (78) <sup>[c]</sup>
16		<b>A2</b>	<b>3h</b> (91)
17	<i>m</i> -HOC <sub>6</sub> H <sub>4</sub> ( <b>1i</b> )	<b>A1</b>	<b>3i</b> (74) <sup>[c]</sup>
18		<b>A2</b>	<b>3i</b> (98)
19	<i>m</i> -FC <sub>6</sub> H <sub>4</sub> ( <b>1j</b> )	<b>A1</b>	<b>3j</b> (67)
20		<b>A2</b>	<b>3j</b> (77)
21	<i>m</i> -ClC <sub>6</sub> H <sub>4</sub> ( <b>1k</b> )	<b>A1</b>	<b>3k</b> (60)
22		<b>A2</b>	<b>3k</b> (83)
23	<i>o</i> -MeOC <sub>6</sub> H <sub>4</sub> ( <b>1l</b> )	<b>A1</b>	<b>3l</b> (30)
24		<b>A2</b>	<b>3l</b> (24)
25	3-thienyl ( <b>1m</b> )	<b>A1</b>	<b>3m</b> (84)
26		<b>A2</b>	<b>3m</b> (86)
27	cyclopropyl ( <b>1n</b> )	<b>A1</b>	<b>3n</b> (46) <sup>[c]</sup>
28		<b>A2</b>	<b>3n</b> (35)

<sup>[a]</sup> **2a/1a–n** = 2:1.

<sup>[b]</sup> Isolated yields.

<sup>[c]</sup> Ref.<sup>[3]</sup>

entries 6, 14, and 24). In the case of **1n**, a lower yield was obtained (Table 2, entry 28). Cyclobutene **3a** was also obtained in 95% yield by performing the reaction on a larger scale (2.0 mmol). Generating *in situ* **A2** by simple mixing of (*t*-BuXPhos)gold(I) chloride and NaBAR<sub>4</sub><sup>F</sup> did not mean any drop in the yield.

Improved yields were also obtained in general when phenylacetylene (**1a**) was used with different alkenes (Table 3). The reaction can also be extended to allylsilane **2d**, allyl ether **2e** and allyl silyl ether **2f**, although yields were modest due to the lower nucleophilicity of these alkenes.

The yield in the macrocyclization of 1,14-enyne **10** to form 13-membered derivative **11** was also improved from 57% using **A1** to 82% with **A2** (Scheme 3).<sup>[7]</sup>

We also explored the influence of the counterion in the intermolecular [2+2+2] cycloaddition of alkynes

**Table 3.** Intermolecular gold(I)-catalyzed [2+2] cycloaddition between phenylacetylene (**1a**) and alkenes **2b–f**.<sup>[a]</sup>

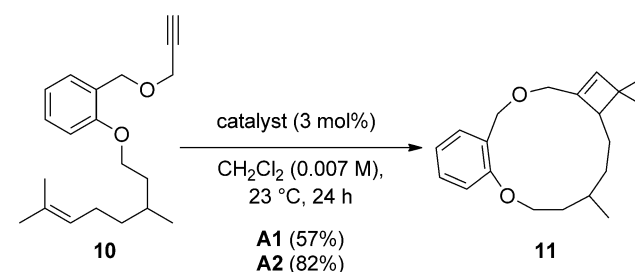
Entry	R <sup>1</sup> , R <sup>2</sup> , R <sup>3</sup>	Catalyst	Product (Yield [%])
1	<b>2b</b>	<b>A1</b>	<b>3o</b> (74) <sup>[b,c]</sup>
2		<b>A2</b>	<b>3o</b> (79) <sup>[b]</sup>
3	<b>2c</b>	<b>A1</b>	<b>3p</b> (53) <sup>[b,c]</sup>
4		<b>A2</b>	<b>3p</b> (69) <sup>[b]</sup>
5	<b>2d</b>	<b>A1</b>	<b>3q</b> (48) <sup>[d]</sup>
6		<b>A2</b>	<b>3q</b> (71) <sup>[d]</sup>
7	<b>2e</b>	<b>A1</b>	<b>3r</b> (26) <sup>[d]</sup>
8		<b>A2</b>	<b>3r</b> (31) <sup>[d]</sup>
9	<b>2f</b>	<b>A1</b>	<b>3s</b> (21) <sup>[d]</sup>
10		<b>A2</b>	<b>3s</b> (31) <sup>[d]</sup>

<sup>[a]</sup> **2b–f/1a** = 2:1.

<sup>[b]</sup> Isolated yields.

<sup>[c]</sup> Ref.<sup>[3]</sup>

<sup>[d]</sup> Yield determined by <sup>1</sup>H NMR using 1,4-diacetylbenzene as internal standard.

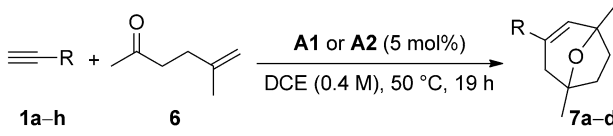


**Scheme 3.** Gold(I)-catalyzed macrocyclization of a 1,14-enyne.

with oxoalkene **6** to furnish 8-oxabicyclo[3.2.1]oct-3-enes **7a–d** using **A1** and **A2**. For this more challenging cascade reaction, we could also observe a moderate improvement of the yields using catalyst **A2** (Table 4, entries 2, 4, 6, and 8).

To define the role of the anion in intermolecular reactions, we studied experimentally the mechanism of the [2+2] cycloaddition between alkynes and alkenes. According to previous theoretical work,<sup>[7,12]</sup> the catalytic cycle for the [2+2] cycloaddition of alkynes with alkenes was expected to proceed by a rate-determining attack of the electron-rich alkene to the ( $\eta^2$ -alkyne)gold(I) complex **8** forming the cyclopropyl

**Table 4.** Intermolecular gold(I)-catalyzed cyclization of 5-methylhex-5-en-2-one (**6**) with terminal alkynes (**1a–h**).<sup>[a]</sup>

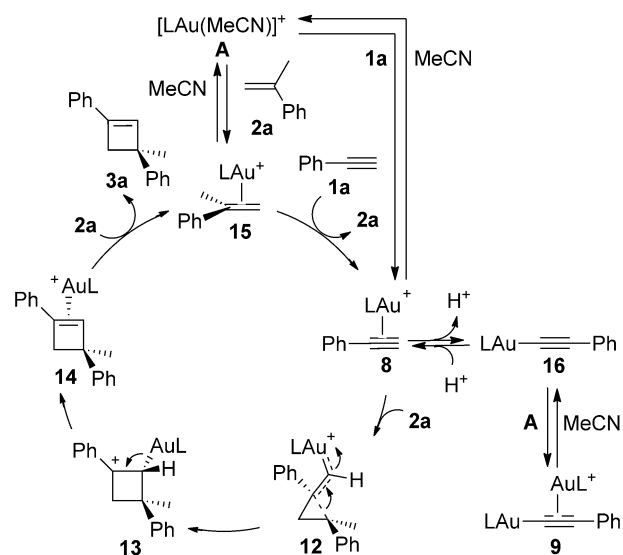


Entry	R	Catalyst	Product (Yield [%]) <sup>[b]</sup>
1	Ph ( <b>1a</b> )	<b>A1</b>	<b>7a</b> (68) <sup>[c]</sup>
2		<b>A2</b>	<b>7a</b> (72)
3	<i>p</i> -ClC <sub>6</sub> H <sub>4</sub> ( <b>1e</b> )	<b>A1</b>	<b>7b</b> (51) <sup>[c]</sup>
4		<b>A2</b>	<b>7b</b> (62)
5	<i>m</i> -HOC <sub>6</sub> H <sub>4</sub> ( <b>1i</b> )	<b>A1</b>	<b>7c</b> (65) <sup>[c]</sup>
6		<b>A2</b>	<b>7c</b> (81)
7	<i>m</i> -Tol ( <b>1h</b> )	<b>A1</b>	<b>7d</b> (70) <sup>[c]</sup>
8		<b>A2</b>	<b>7d</b> (72)

<sup>[a]</sup> **6/1a–h** = 1:3.5.

<sup>[b]</sup> Isolated yields.

<sup>[c]</sup> Ref.<sup>[7]</sup>



**Scheme 4.** Mechanism of the [2+2]cycloaddition between alkynes and alkenes considering all the gold(I) species in equilibrium.

gold(I) carbene **12** (Scheme 4). Then, the ring expansion occurs to form benzylic carbocation **13**, which forms cyclobutene **3a** after demetallation. An associative ligand exchange between ( $\eta^2$ -cyclobutene)gold(I) complex **14** and the starting alkyne closes the catalytic cycle, regenerating **8**.

However, in our previous study on the [2+2+2]cycloaddition of alkynes with oxoalkenes,<sup>[7]</sup> we had observed that the formation of the ( $\eta^2$ -alkyne)gold(I) complex **8a** is complicated by the competitive formation of  $\sigma,\pi$ -digold(I) alkyne complex **9a** (Scheme 2). Therefore, we determined the order of the reagents in the rate equation to gain further insight in the mecha-

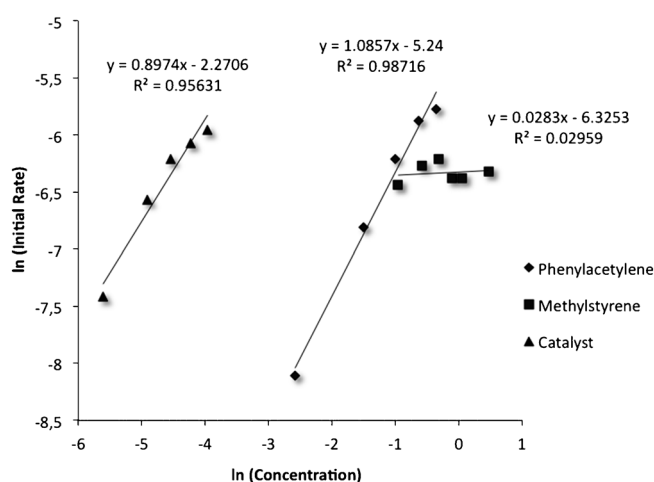


**Figure 2.** Order of the reagents in the [2+2]cycloaddition between phenylacetylene (**1a**) and  $\alpha$ -methylstyrene (**2a**) with complex **A2**.

nism. Initial rates were calculated for each component by <sup>1</sup>H NMR using diphenylmethane as internal standard (Figure 2). First order was observed for both the alkyne **1a** and the gold(I) catalyst **A2**, whereas the reaction showed zero order dependence for the alkene **2a**.

These results are consistent with a scenario in which the actual rate-determining step is the ligand exchange to generate the active species **8** (Scheme 4). Complex **A** undergoes ligand exchange with **2a** forming **15**. Generation of **8** is the slowest step due to its instability and rapid evolution to **9** or **3a**.

Monitoring the [2+2]cycloaddition reaction by <sup>1</sup>H NMR showed a significant dependence on the anion (Figure 3). Besides the difference in the final yields, the reaction rate increases with the bulkiness

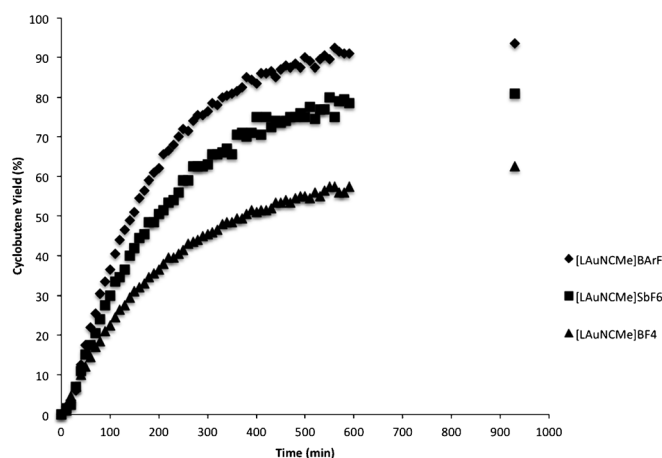
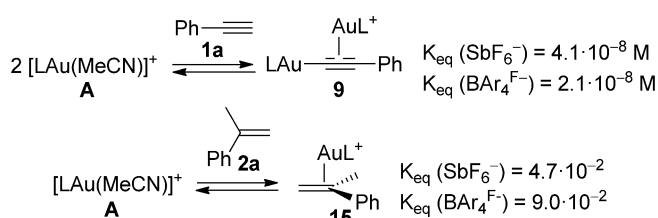


**Figure 3.** Kinetics of the [2+2]cycloaddition between phenylacetylene (**1a**) and  $\alpha$ -methylstyrene (**2a**) with different gold(I) complexes (L = *t*-BuXPhos).

and the softness of the counterion:  $\text{BAr}_4^{\text{F}^-} > \text{SbF}_6^- > \text{BF}_4^-$ .

Analysis of the reaction mixture by  $^{31}\text{P}$  NMR showed only the (alkene)gold(I) complex **15** and the digold complex **9**. The ratio between these species  $[\mathbf{15}]/[\mathbf{9}]$  increased following the same trend:  $\text{BAr}_4^{\text{F}^-} (\mathbf{b}) > \text{SbF}_6^- (\mathbf{a}) > \text{BF}_4^- (\mathbf{c})$ . Thus,  $[\mathbf{15}]/[\mathbf{9}]$  drops from 115 ( $\text{BAr}_4^{\text{F}^-}$ ) to 30 ( $\text{SbF}_6^-$ ) and finally to 4 for  $\text{BF}_4^-$  resulting in a smaller reservoir of the cationic gold(I) species.

The equilibrium constants for the formation of **9** and **15** from **A1** and **A2** were also determined, endothermic and exothermic, respectively (Scheme 5). For-

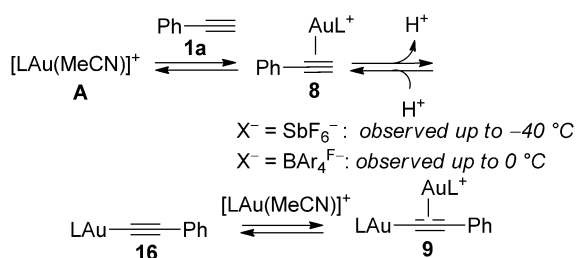


**Scheme 5.** Determination of the equilibrium constants from **A** to **9** and **15**.

mation of digold(I) complex with  $\text{SbF}_6^-$  (**9a**) anion is more favored than with  $\text{BAr}_4^{\text{F}^-}$  (**9b**), probably due to the minor stability of the bulkier conjugated acid. We also checked that **A2** binds stronger to **2a** than **A1**.

These results suggest that when  $\text{BAr}_4^{\text{F}^-}$  is used, the concentration of catalytically active species **8b** ( $\text{BAr}_4^{\text{F}^-}$  as counteranion) is higher than with  $\text{SbF}_6^-$  (**8a**). We also studied the evolution of the gold(I) species formed with **A1** or **A2** and **1a** from  $-60$  to  $20^\circ\text{C}$  by  $^{31}\text{P}$  NMR. With **A1**, the digold(I) complex **9a** was observed from  $-60^\circ\text{C}$ , becoming the only species at  $-20^\circ\text{C}$  (Scheme 6). However, in the case of **A2**, the corresponding digold(I) complex **9b** was not observed until  $0^\circ\text{C}$ . Furthermore, the catalytically active species **8b** was clearly observed up to the same temperature.

Complexes **15b** and **9b** (Figure 4) could be isolated and were fully characterized by X-ray crystallography.<sup>[13]</sup> The main divergence between **9a** and **9b** in the



**Scheme 6.** Gold(I) species formed between phenylacetylene (**1a**) and **A1** or **A2** from 213 to 293 K.

solid state (Figure 4b and c, respectively) is the radically different position of the counterions. Whereas  $\text{BAr}_4^{\text{F}^-}$  is located alongside the phenylacetylene moiety in the same plane,  $\text{SbF}_6^-$  is placed between both gold atoms bending slightly the cation entity. Thus, the angle of the  $\pi$ -coordinated gold(I), the alkyne and the counterion is  $130.3^\circ$  for  $\text{BAr}_4^{\text{F}^-}$  (Au–B 10.22 Å) and  $77.3^\circ$  for  $\text{SbF}_6^-$  (Au–Sb 8.23 Å) and the angle of the  $\sigma$ -gold is  $210.0^\circ$  for  $\text{BAr}_4^{\text{F}^-}$  (Au–B 11.52 Å) and  $60.6^\circ$  for  $\text{SbF}_6^-$  (Au–Sb 7.34 Å). Complex **16** was independently prepared by reaction of the neutral gold(I) complex with lithium phenylacetylide and its structure was determined by X-ray diffraction.<sup>[13,14]</sup>

We performed DFT calculations of the key complexes [*t*-BuXPhosAu( $\eta^2$ -phenylacetylene)]X **8** ( $\text{X} = \text{BF}_4^-, \text{SbF}_6^-, \text{BAr}_4^{\text{F}^-}$ ) [M06, 6-31G(d) (C, H, P, B, F) and SDD (Au, Sb),  $\text{CH}_2\text{Cl}_2$ ]. First, we evidenced the steric congestion around the substrate hampering its deprotonation depending on the counterion. We analyzed the charge distribution by electron density from total SCF density mapped with ESP ( $\rho = 0.03 \text{ e}\text{\AA}^{-3}$ ) and the positive charge is widely distributed around the ligand instead of being concentrated in the metal center (Figure 5). We also checked the pattern between the bulkiness of the counterion and the acidity of phenylacetylene by determining the Mulliken atomic charges. The electron density decreases with the anion size:  $\text{BF}_4^- < \text{SbF}_6^- < \text{BAr}_4^{\text{F}^-}$ , although the differences are modest: 0.250 for  $\text{BF}_4^-$  (**8c**), 0.243 for  $\text{SbF}_6^-$  (**8a**) and 0.237 for  $\text{BAr}_4^{\text{F}^-}$  (**8b**). Presumably, the large cation forms a more stable complex **8** with a softer counterion as  $\text{BAr}_4^{\text{F}^-}$ .

Finally, we performed some additional experiments to exclude other mechanistic pathways.<sup>[14]</sup> We started by reacting the isolable intermediates under stoichiometric conditions with  $\alpha$ -methylstyrene (**2a**). Neither complex **9** nor **16** reacted with **2a** in  $\text{CH}_2\text{Cl}_2$  at  $23^\circ\text{C}$  for 8 h in the absence or presence of **A2** as a catalyst. On the other hand, complex **15b** (Figure 4) reacts with **1a** to form cyclobutene **3a** in 72% ( $\text{CH}_2\text{Cl}_2$ ,  $23^\circ\text{C}$ , 8 h) therefore that equilibrium is not inhibiting the process.

Complex **16** is not catalytically active for the formation of **3a** by [2+2] cycloaddition, although the activity is restored upon addition of  $\text{HSbF}_6$ , which cleaves the Au–C bond generating the gold(I) catalyst (Table 5, entries 1 and 2). More significantly, as we observed before in another context,<sup>[7]</sup> digold complexes **9a** and **9b** are very poor catalysts for the [2+2] cycloaddition between **1a** with **2a** (Table 5, entries 3 and 4), although the reaction proceeds smoothly after addition  $\text{HSbF}_6$  (Table 5, entry 5).

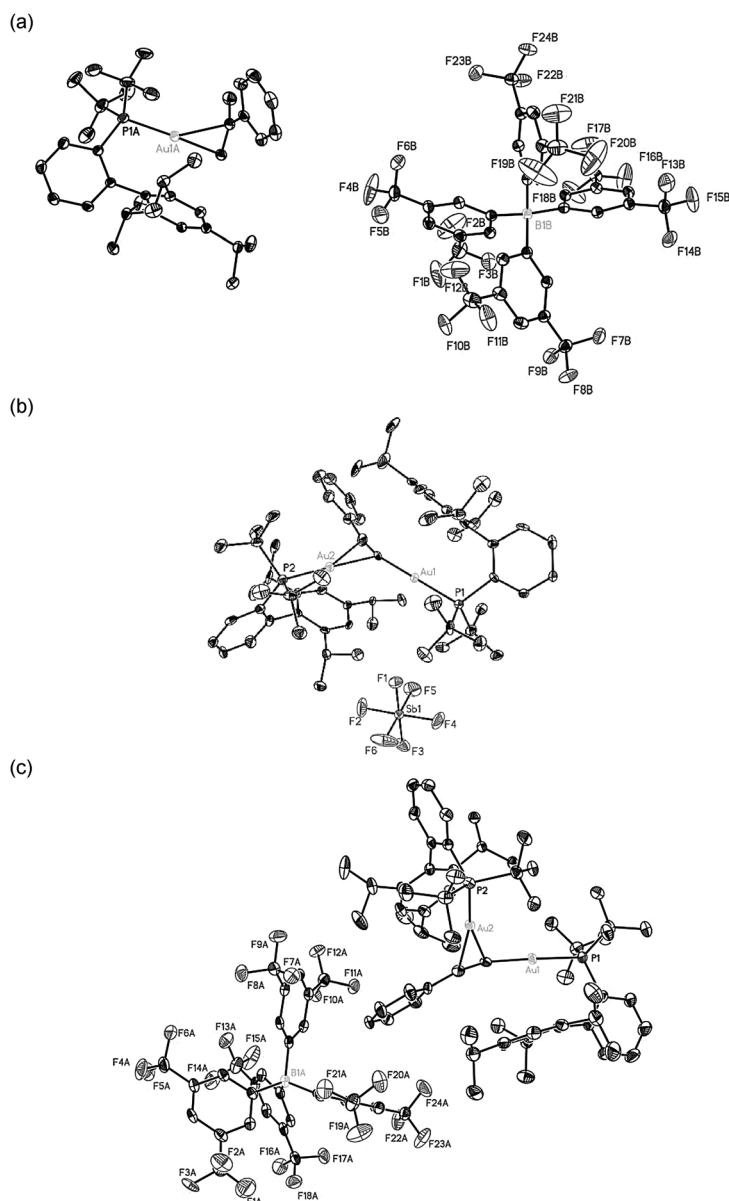


**Figure 4.** X-Ray crystal structures: (a)  $\alpha$ -methylstyrene gold(I) complex **15b**, (b)  $[(t\text{-BuXPhosAu})_2\text{C}\equiv\text{CPh}]^+[\text{SbF}_6]^-$  **9a** (taken from ref.<sup>[7]</sup>) and (c)  $[(t\text{-BuXPhosAu})_2\text{C}\equiv\text{CPh}]^+[\text{BAR}_4^{\text{F}}]^-$  **9b**. ORTEP plot (50% thermal ellipsoids). Hydrogens are omitted for clarity.

## Conclusions

We have designed a new generation of gold(I) complexes bearing  $\text{BAR}_4^{\text{F}-}$  as counterion [ $\text{BAR}_4^{\text{F}-} = 3,5$ -bis(trifluoromethyl)phenylborate]. These have proven to be more efficient in different intermolecular gold(I)-catalyzed reactions, improving the yields between 10 and 30%. We have then studied in detail the subtle anion effects in the gold(I)-catalyzed [2+2] cycloaddition of terminal alkynes with alkenes, which sum up in a substantial decrease in the formation of unproductive  $\sigma,\pi$ -(alkyne)digold(I) complex when the  $\text{BAR}_4^{\text{F}-}$  anion is used.

Our kinetic study of the gold(I)-catalyzed [2+2] cycloaddition reaction of terminal alkynes with alkenes is consistent with a scenario in which the rate-determining step is the first ligand exchange of  $[\text{LAu}(\text{MeCN})]\text{X}$  to generate the active  $(\eta^2\text{-phenylacetylene})\text{gold(I)}$  complex, which is more stable with softer counterions according to DFT calculations. From a general practical perspective, we have found that the best results in intermolecular gold(I)-catalyzed reactions are obtained using  $[(t\text{-BuXPhosAu})(\text{MeCN})]\text{BAR}_4^{\text{F}}$  as catalyst.

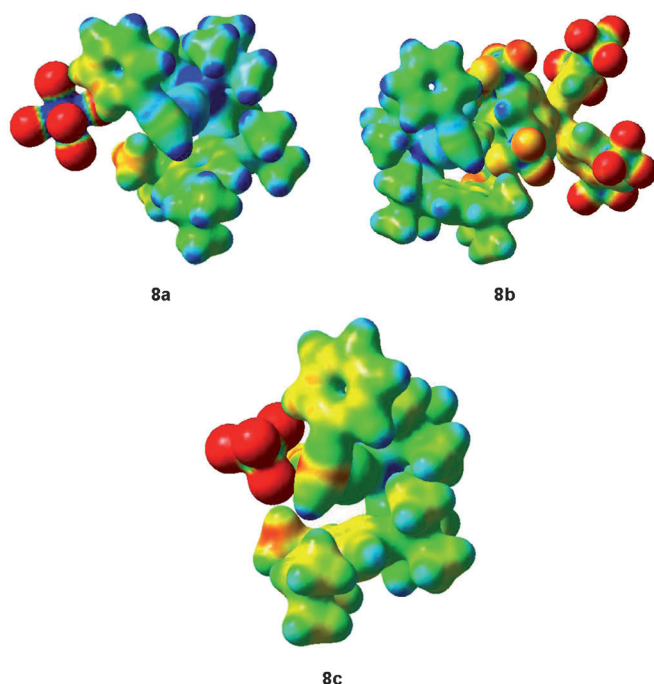
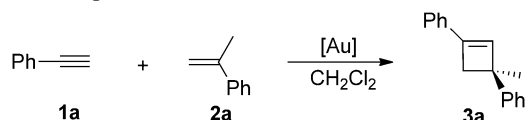


**Figure 5.** Electron density from total SCF density mapped with ESP ( $\rho = 0.03 \text{ e } \text{\AA}^{-3}$ ) for complexes **8** [*t*-BuXPhosAu( $\eta^2$ -phenylacetylene)X, X = SbF<sub>6</sub><sup>−</sup> (**8a**), BAr<sub>4</sub><sup>F−</sup> (**8b**), and BF<sub>4</sub><sup>−</sup> (**8c**)].

**Table 5.** Regeneration of the catalytic activity in the intermolecular gold(I)-catalyzed [2+2]cycloaddition between **1a** and **2a** in the presence of a Brønsted acid.<sup>[a]</sup>



Entry	[Au] (mol%)	Additive (mol%)	Yield [%] <sup>[b]</sup>
1	<b>16</b> (3)	–	–
2	<b>16</b> (3)	HSbF <sub>6</sub> ·6H <sub>2</sub> O (3)	75
3	<b>9a</b> (1.5)	–	13
4	<b>9b</b> (1.5)	–	13
5	<b>9a</b> (1.5)	HSbF <sub>6</sub> ·6H <sub>2</sub> O (1.5%)	70

<sup>[a]</sup> 23 °C, 8 h.

<sup>[b]</sup> Yield determined by <sup>1</sup>H NMR using 1,4-diacetylbenzene as internal standard.

## Experimental Section

### Procedure for the Synthesis of Gold(I) Complex **A2**

Chloro[(2',4',6'-triisopropyl-1,1'-biphenyl-2-yl)di-*tert*-butylphosphine]gold(I) (100.0 mg, 0.152 mmol) and acetonitrile (9.5  $\mu$ L, 0.183 mmol) were dissolved in dichloromethane (6.6 mL). Then, sodium tetrakis[3,5-bis(trifluoromethyl)phenyl]borate (135.0 mg, 0.152 mmol) was added and the reaction mixture was stirred at room temperature for 30 min. The crude was filtered through Celite, then Teflon 0.22 and

concentrated to obtain a white powder; yield: 224 mg (97%).

### Procedure for the Synthesis of Cyclobutenes (**3**)

Alkyne (1 equiv.) and alkene (2 equiv.) were dissolved in dichloromethane (0.48 M) and the cationic gold(I) catalyst (3 mol%) was added. The reaction mixture was stirred at room temperature until no alkyne was observed by TLC. Then, it was quenched by adding a drop of a solution of Et<sub>3</sub>N in cyclohexane (1 M) and the solvent was removed. Preparative TLC was used to purify the resulting cyclobutenes.

## Acknowledgements

We thank the MICINN (CTQ2010-16088/BQU and FPI fellowship to A. H.), the AGAUR (project 2009 SGR 47 and Beatriu de Pinós postdoctoral fellowship to D. L.), the MEC (FPU fellowship to C. O.), the European Research Council (Advanced Grant No. 321066), and the ICIQ Foundation for financial support. We also thank the ICIQ X-ray diffraction, the Nuclear Magnetic Resonance and the Spectroscopic and Kinetics units.

## References

- a) L. Zhang, J. Sun, S. A. Kozmin, *Adv. Synth. Catal.* **2006**, *348*, 2271–2296; b) A. S. K. Hashmi, G. J. Hutchings, *Angew. Chem.* **2006**, *118*, 8064–8105; *Angew. Chem. Int. Ed.* **2006**, *45*, 7896–7936; c) A. Fürstner, P. W. Davies, *Angew. Chem.* **2007**, *119*, 3478–3519; *Angew. Chem. Int. Ed.* **2007**, *46*, 3410–3449; d) A. S. K. Hashmi, *Chem. Rev.* **2007**, *107*, 3180–3211; e) Z. Li, C. Brouwer, C. He, *Chem. Rev.* **2008**, *108*, 3239–3265; f) A. Arcadi, *Chem. Rev.* **2008**, *108*, 3266–3325; g) E. Jiménez-Núñez, A. M. Echavarren, *Chem. Rev.* **2008**, *108*, 3326–3350; h) D. J. Gorin, B. D. Sherry, F. D. Toste, *Chem. Rev.* **2008**, *108*, 3351–3378; i) V. Michelet, P. Y. Toullec, J.-P. Genêt, *Angew. Chem.* **2008**, *120*, 4338–4386; *Angew. Chem. Int. Ed.* **2008**, *47*, 4268–4315; j) A. Fürstner, *Chem. Soc. Rev.* **2009**, *38*, 3208–3221; k) C. Aubert, L. Fensterbank, P. Garcia, M. Malacria, A. Simonneau, *Chem. Rev.* **2011**, *111*, 1954–1993; l) N. Krause, C. Winter, *Chem. Rev.* **2011**, *111*, 1994–2009.
- For selected examples, see: a) C. Ferrer, C. H. M. Amijs, A. M. Echavarren, *Chem. Eur. J.* **2007**, *13*, 1358–1373; b) R. B. Dateer#, B. S. Shaibu, R. S. Liu, *Angew. Chem.* **2012**, *124*, 117–121; *Angew. Chem. Int. Ed.* **2012**, *51*, 113–117; c) H.-S. Yeom, J. Koo, H.-S. Park, Y. Wang, Y. Liang, Z.-X. Yu, S. Shin, *J. Am. Chem. Soc.* **2012**, *134*, 208–211; d) S. Kramer, T. Skrydstrup, *Angew. Chem.* **2012**, *124*, 4759–4762; *Angew. Chem. Int. Ed.* **2012**, *51*, 4681–4684; e) Y. Luo, K. Ji, Y. Li, L. Zhang, *J. Am. Chem. Soc.* **2012**, *134*, 17412–17415.
- V. López-Carrillo, A. M. Echavarren, *J. Am. Chem. Soc.* **2010**, *132*, 9292–9294.
- Conceptually analogous macrocyclization by cycloaddition of alkynes with alkenes, see: C. Obradors, D.

- Lebœuf, J. Aydin, A. M. Echavarren, *Org. Lett.* **2013**, *15*, 1576–1579.
- [5] N. Huguët, D. Lebœuf, A. M. Echavarren, *Chem. Eur. J.* **2013**, *19*, 6581–6585.
- [6] First example of an intramolecular gold-catalyzed formation of phenol with a furan and an alkyne, see: a) A. S. K. Hashmi, E. Kurpejovic, M. Wölflé, W. Frey, J. W. Bats, *Adv. Synth. Catal.* **2007**, *349*, 1743–1750; b) A. S. K. Hashmi, M. C. Blanco, E. Kurpejovic, W. Frey, J. W. Bats, *Adv. Synth. Catal.* **2006**, *348*, 709–713; c) A. S. K. Hashmi, M. C. Blanco, *Eur. J. Org. Chem.* **2006**, 4340–4342.
- [7] C. Obradors, A. M. Echavarren, *Chem. Eur. J.* **2013**, *19*, 3547–3551.
- [8] a) C. Wei, C. J. Li, *J. Am. Chem. Soc.* **2003**, *125*, 9584–9585; b) V. Lavallo, G. D. Frey, S. Kousar, B. Donnadiou, G. Bertrand, *Proc. Natl. Acad. Sci. USA* **2007**, *104*, 13569–13573; c) P. H. Y. Cheong, P. Morganelli, M. R. Luzung, K. N. Houk, F. D. Toste, *J. Am. Chem. Soc.* **2008**, *130*, 4517–4526; d) T. N. Hooper, M. Green, C. A. Russell, *Chem. Commun.* **2010**, *46*, 2313–2315; e) A. Simonneau, F. Jaroschik, D. Lesage, M. Karanik, R. Guillot, M. Malacria, J.-C. Tabet, J.-P. Goddard, L. Fensterbank, V. Gandon, Y. Gimbert, *Chem. Sci.* **2011**, *2*, 2417–2422; f) A. Griirane, H. Garcia, A. Corma, E. Álvarez, *ACS Catal.* **2011**, *1*, 1647–1653; g) T. J. Brown, R. A. Widenhofer, *Organometallics* **2011**, *30*, 6003–6009; h) M. Raducan, M. Moreno, C. Bour, A. M. Echavarren, *Chem. Commun.* **2012**, *48*, 52–54; i) A. S. K. Hashmi, T. Lauterbach, P. Nösel, M. H. Vilhelmsen, M. Rudolph, F. Rominger, *Chem. Eur. J.* **2013**, *19*, 1058–1065; j) A. Gómez-Suárez, S. Dupuis, A. M. Z. Slawin, S. P. Nolan, *Angew. Chem.* **2013**, *125*, 972–976; *Angew. Chem. Int. Ed.* **2013**, *52*, 938–942; k) A. Zhdanko, M. Ströbele, M. E. Maier, *Chem. Eur. J. Chem. -Eur. J.* **2012**, *18*, 14732–14744; l) A. S. K. Hashmi, I. Braun, P. Nösel, J. Schädlich, M. Wieteck, M. Rudolph, F. Rominger, *Angew. Chem.* **2012**, *124*, 4532–4536; *Angew. Chem. Int. Ed.* **2012**, *51*, 4456–4460; m) B. Rubial, A. Ballesteros, J. M. González, *Adv. Synth. Catal.* **2013**, *355*, 3337–3343.
- [9] A gold(I) carbene with tetrakis[3,5-bis(trifluoromethyl)phenyl]borate as the counterion has been reported to undergo C–B cleavage to form an aryl-gold(I) complex due to the high electrophilicity of the metal center. However, we never observed this behavior with complex **A2**: S. G. Weber, D. Zahner, F. Rominger, B. F. Straub, *Chem. Commun.* **2012**, *48*, 11325–11327.
- [10] P. Pérez-Galán, N. Delpont, E. Herrero-Gómez, F. Maseras, A. M. Echavarren, *Chem. Eur. J.* **2010**, *16*, 5324–5332.
- [11] C. H. M. Amijs, V. López-Carrillo, M. Raducan, P. Pérez-Galán, C. Ferrer, A. M. Echavarren, *J. Org. Chem.* **2008**, *73*, 7721–7730.
- [12] a) C. Nieto-Oberhuber, S. López, M. P. Muñoz, D. J. Cárdenas, E. Buñuel, C. Nevado, A. M. Echavarren, *Angew. Chem.* **2005**, *117*, 6302–6304; *Angew. Chem. Int. Ed.* **2005**, *44*, 6146–6148; b) A. Escribano-Cuesta, P. Pérez-Galán, E. Herrero-Gómez, M. Sekine, A. A. C. Braga, F. Maseras, A. M. Echavarren, *Org. Biomol. Chem.* **2012**, *10*, 6105–6111.
- [13] CCDC 953708 (**12b**), CCDC 953710 (**9b**), and CCDC 953709 (**16**) contain the supplementary crystallographic data for this paper. These data can be obtained free of charge from The Cambridge Crystallographic Data Centre via [www.ccdc.cam.ac.uk/data\\_request/cif](http://www.ccdc.cam.ac.uk/data_request/cif).
- [14] See the Supporting Information for details.